

# COMSOL's New Thermoacoustics Interface and Computationally Efficient Alternative Formulations for FEM

W.R. Kampinga<sup>\*1</sup> and Y.H. Wijnant<sup>2</sup>

<sup>1</sup>Reden B.V., Hengelo, Netherlands, <sup>2</sup>University of Twente, Enschede, Netherlands

\*Corresponding author: [www.reden.nl](http://www.reden.nl), [r.kampinga@reden.nl](mailto:r.kampinga@reden.nl)

**Abstract:** Three efficient alternatives to the model in COMSOL's thermoacoustics interface are presented. The higher efficiency of these models are explained from theory and are demonstrated by means of two examples.

**Keywords:** Thermoacoustics, PDE, Efficient, Transducer.

## 1. Introduction

The acoustics module of COMSOL 4.2 contains a thermoacoustics interface. This interface can, for example, be used to model miniature acoustic transducers. Different than in normal (isentropic/lossless) acoustics, the thermoacoustic formulation takes the dissipative effects of viscous shear and heat conduction into account. These effects cannot be neglected in acoustic wave propagation through narrow geometries. COMSOL's new interface facilitates accurate and easy to use modeling of viscothermal<sup>1</sup> acoustic problems.

The *full* viscothermal acoustic formulation used by COMSOL does have the disadvantage of high a computational cost. More efficient *reduced* formulations are available in the literature, although most can only be applied to a limited range of geometries. This paper presents three alternative formulations, that could be used to speed up the calculation time, (or to increase the problem size). One of these alternatives can be applied to an geometry.

The calculations, figures and tables in this paper have been published previously in [1,2] in a more elaborate form. This paper is a brief overview of the results from that research.

All results in this paper were obtained with COMSOL 3.5a, using the PDE application mode. COMSOL 4.2 was not yet released at the time this research was done.

## 2. Viscothermal acoustics

<sup>1</sup> The terms viscothermal acoustics and thermoacoustics are used interchangeably in this paper.

The viscous shear damping in viscothermal acoustics typically occurs near no-slip boundaries. Likewise, the damping by heat conduction typically occurs near isothermal boundaries. The formed viscous and thermal boundary layers have comparable thicknesses that are much smaller than the acoustic wave length (in air at audible frequencies). Figure 1 compares these frequency ( $f$ ) dependent length scales ( $\lambda_\phi$ ). This difference in length scales makes *full* viscothermal acoustic models inefficient, because a large number of elements is needed in the boundary layers. On the other hand, this large length scale difference stands at the basis of the theory of the *reduced* models.

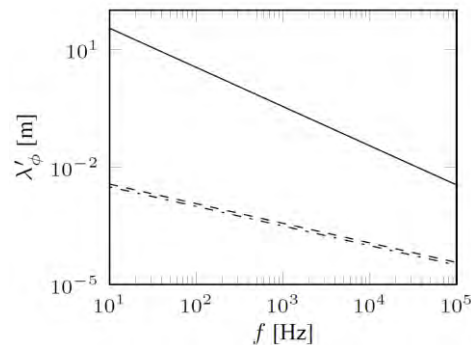


**Figure 1.** Characteristic length scales for air: acoustic wave length (solid), viscous boundary layer thickness (dash-dot) and thermal boundary layer thickness (dashed).

Following from the description above, two distinct regions can typically be distinguished in a viscothermal acoustic solution:

1. A boundary layer in which the viscothermal dissipative effects are significant.
2. A bulk region that may as well be modeled using normal isentropic acoustics<sup>2</sup>.

Figure 2 schematically shows these regions. In very small or narrow domains, the bulk region can disappear completely. In the other extreme, in very large domains, the boundary

<sup>2</sup> COMSOL's new thermoacoustics interface provides boundary conditions to couple isentropic acoustics and viscothermal acoustics to reduce the computational cost.

layer can become insignificant and viscothermal effects might be neglected completely, as is done in standard isentropic acoustics.

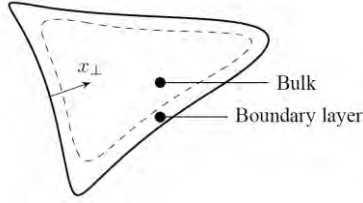


**Figure 2.** Bulk and boundary layer regions in a viscothermal acoustic domain.

### 3. Four models

Four different models of viscothermal acoustics are compared in this paper. These formulations are briefly introduced here without mathematical derivations and without boundary conditions. This section is aimed to explain the efficiency by showing the PDE's and the data flow in the four models. The four models are

1. FLNS model (COMSOL's model), [2,3,8].
2. Bossart/Cremer model, [4,2].
3. LRF model, [6,3,2].
4. SLNS model, [1,2].

#### 3.1 FLNS model (COMSOL's model)

The 'Full Linearized Navier-Stokes' (FLNS) model is the viscothermal acoustic model implemented in the PDE application mode of COMSOL 3.5a. The FLNS model is equivalent to the new thermoacoustics interface in COMSOL 4.2.

The governing equations are the linear time harmonic PDEs

$$\begin{aligned} i\omega\rho_0\mathbf{v} - \nabla \cdot \boldsymbol{\tau} + \nabla p &= 0, \\ i\omega\rho_0 C_p T + \nabla \cdot \mathbf{q} - i\omega p &= 0, \\ \nabla \cdot \mathbf{v} - i\omega \frac{T}{T_0} + i\omega \frac{p}{p_0} &= 0, \end{aligned}$$

with

$$\begin{aligned} \nabla \cdot \boldsymbol{\tau} &= (\lambda + \mu)\nabla(\nabla \cdot \mathbf{v}) + \mu\Delta\mathbf{v}, \\ \nabla \cdot \mathbf{q} &= -\kappa\Delta T, \end{aligned}$$

in which the symbols  $\rho_0$ ,  $T_0$ ,  $p_0$ , and  $C_p$  denote the quiescent density, quiescent temperature, quiescent pressure and the specific heat at constant pressure;  $\lambda$ ,  $\mu$  and  $\kappa$  denote the second viscosity, dynamic viscosity and heat conduction coefficient;  $\boldsymbol{\tau}$  and  $\mathbf{q}$  denote the viscous tensor and the heat flux vector;  $\mathbf{v}$ ,  $p$

and  $T$  denote the velocity, pressure and temperature perturbation fields; and  $\nabla$ ,  $\nabla \cdot$  and  $\Delta$  are the gradient, divergence and Laplace operators.

The FLNS is computationally costly for two reasons

- It contains five (four in 2D) coupled fields ( $v_1, v_2, v_3, T, p$ ) of which four (three in 2D) are quadratic [3,8];  $p$  is linear.
- The mesh must be very fine near no-slip/isothermal boundaries to be able to accurately solve for the viscous and thermal boundary layers and the resulting acoustic damping.

The FLNS model is widely applicable. Practically any geometry can be modeled with this model.

*The FLNS model (COMSOL's model) is widely applicable, but not efficient.*

#### 3.2 Bossart/Cremer model

Bossart presents an efficient model of viscothermal acoustics for the boundary element method in [4]. His model can be applied to finite elements as well. The equation on the domain is essentially the isotropic acoustic Helmholtz equation of the pressure<sup>3</sup>:

$$\Delta p + k_0^2 p = 0,$$

with

$$k_0 \equiv \frac{\omega}{c_0},$$

in which  $k_0$  and  $c_0$  are the acoustic wave number and the speed of sound respectively.

All dissipative viscothermal effects near walls are captured in the *acoustic* boundary condition that is of the impedance type. Bossart's model can be regarded as a generalized application of Cremer's acoustic impedance of a no-slip isothermal wall [5]. Cremer's wall impedance depends on the angle of incidence of the acoustic plane wave. Bossart's model provides a method to estimate this angle in problems with non-plane waves in bounded domains.

<sup>3</sup> Bossart includes a very small bulk damping term in the formulation by using a complex wave number, but its effect is insignificant, especially in small domains.

The model contains two steps:

1. A pressure calculation with an estimated boundary impedance. The angle of incidence is estimated from this solution in a post-processing step; see [2,4].
2. A second pressure calculation with updated boundary impedance values based on the angles of incidence estimated in step 1; see [2,4].

Bossart's model is efficient at roughly twice the computationally cost of isentropic acoustic models, because

- The model contains only the scalar pressure field that must be solved twice.
- The mesh does not have to be fine near walls, because all boundary layer effects are contained in the boundary condition prescribed *at* the wall.

The theory assumes a fully developed boundary layer. This requirement is not met in domains that are (locally) narrower than two boundary layer thicknesses. Therefore, Bossart's model is inaccurate for very small geometries.

*The Bossart/Cremer model is efficient, but not applicable to very small geometries.*

### 3.3 LRF model

The Low Reduced Frequency (LRF) model [6,3,2] describes 1D and 2D waveguides (tubes and layers). The main restriction of the LRF model is that the cross section dimensions should be much smaller than the acoustic wavelength. The pressure is approximately uniform over the cross section under these conditions. This effectively reduces the pressure field to 2D for layers and to 1D for tubes.

The 2D or 1D pressure field is the solution of the Helmholtz PDE

$$\Delta p + k_\ell^2 p = 0,$$

in which the (complex) value of the LRF-wavenumber  $k_\ell$  depends on the cross section of the waveguide. Analytic expressions for  $k_\ell$  are available for layers, and for tubes with round and several other cross-sections. The right-hand side of the pressure PDE is non-zero if the waveguide walls have a (harmonic) velocity that changes the cross-section area.

Reference [2] presents additional information on the LRF model with an emphasis on FEM.

Many other authors have published about the LRF model and waveguide models in general; see [3,6] for example.

The LRF model is very efficient because

- Pressure is the only field variable.
- The mesh is 1D (tubes) or 2D (layers) and only has to capture the acoustic phenomena.

The LRF model can only describe wave guides with a cross section that is much smaller than the acoustic wavelength. Furthermore, the cross section should not change rapidly<sup>4</sup>.

*The LRF model is very efficient but only applicable to narrow wave guides.*

### 3.4 SLNS model

The Sequential Linear Navier-Stokes model is a new development presented in [1,2]. This model does not have the geometric restrictions of Bossart's model and the LRF model and is moderately efficient: less efficient than the Bossart and LRF models and more efficient than the FLNS model.

The SLNS model contains two calculation steps:

1. The 'viscous field'  $\Psi_v$  and 'thermal field'  $\Psi_h$  are solved.
2. The acoustic pressure field is solved from a PDE that depends on  $\Psi_v$  and  $\Psi_h$ .

In step 1, the viscous and thermal fields are the solutions of the uncoupled (non-homogeneous) Helmholtz equations

$$\Delta \Psi_v + k_v^2 \Psi_v = 1,$$

$$\Delta \Psi_h + k_h^2 \Psi_h = 1,$$

with viscous and thermal wave numbers<sup>5</sup>

$$k_v = \sqrt{-i\omega\rho_0/\mu},$$

$$k_h = \sqrt{-i\omega\rho_0 C_p/\kappa},$$

For the boundary conditions see [1,2].

In step 2, the pressure is the solution of the Helmholtz-like PDE

$$\Psi_v \Delta p + \Psi_h' k_0^2 p = 0,$$

with

<sup>4</sup> Acoustic end corrections may be used to reduce errors caused by rapid cross section changes.

<sup>5</sup> These wave numbers squared are purely imaginary, because the viscothermal effects are diffusion processes.

$$\Psi_h' = \gamma - (\gamma - 1)\Psi_h,$$

and the ratio of specific heats  $\gamma$ . For the boundary conditions see [1,2]. The fields  $\Psi_v$ ,  $\Psi_h$  and  $\Psi_h'$  are unity in the bulk region. Therefore, the pressure PDE reduces to the Helmholtz equation of isentropic acoustics in the bulk, as expected.

The SLNS model is moderately efficient because:

- The model contains three *uncoupled* fields;  $\Psi_v$ ,  $\Psi_h$ ,  $p$ .
- The mesh needs to be fine near the walls of the geometry.

The pressure field could be calculated on a coarser mesh, but then a sufficiently large number of integration points is needed such that the viscothermal fields are correctly taken into account.

*The SLNS model is moderately efficient and widely applicable.*

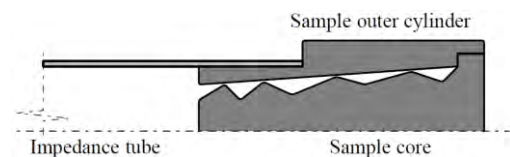
#### 4. Applications

Results from two applications are presented in this section as a demonstration of the four models. Both examples are axi-symmetrical, but the four models are of course not restricted to this modeling space.

##### 4.1 Impedance tube sample

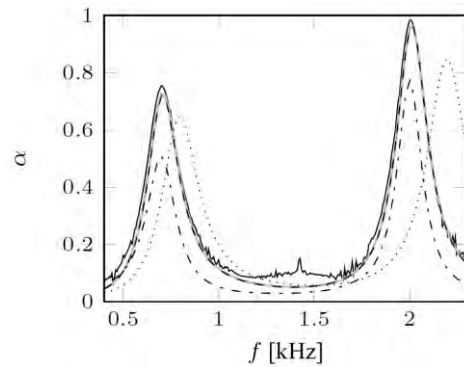
The first application is a sample for an impedance tube. An impedance tube is a waveguide that is used to measure the absorption coefficient of a sample that is located at one end of it. A loudspeaker is located at the opposite end. Two microphones in the impedance tube are used for the absorption measurements; see for example [9].

Figure 3 shows the geometry of the sample. It is made out of two parts: the core and the outer (conical) cylinder. The length of the sample is 10 cm which is the order of the acoustic length scale in the problem. The narrowest passages are approximately 1mm, which is in the order of the viscous and thermal length scales.



**Figure 3.** Axi-symmetric impedance tube sample geometry.

The absorption coefficients  $\alpha$  from a measurement and from calculations with the four FEM models are shown in Figure 4. The FLNS and SLNS model match the measurement quite well. Bossart's model predicts the resonance frequencies well, but underestimates the amount of damping. This error is expected because the narrowest passages in the sample are smaller than twice the boundary layer thickness. The LRF model is not accurate either. This could have been expected as well, because the sample's cross section is not smoothly varying<sup>6</sup>.



**Figure 4.** Absorption coefficient of the impedance tube sample: measurement (solid), FLNS model (grey); SLNS model (dashed), Bossart's model (dash-dot); LRF model (dotted).

The calculation time (per frequency) and the number of degrees of freedom for the four models is listed in Table 1. Although Bossart's model and the LRF model are inaccurate for this problem, the table still gives a correct representation of the differences in efficiency that can be expected. The LRF model is relatively slow in this example because the sample has an annular cross section that is described by unusually complicated analytic functions. Furthermore, 3D models typically shown larger differences than this 2D axi-symmetric model. The FLNS model and SLNS model used the same FEM mesh, while Bossart's model uses a coarser mesh.

**Table 1.** Efficiency of the four impedance tube sample models.

Model	time [s]	# of DOFs
FLNS	44	$584 \cdot 10^3$
SLNS	6.8	$(110+55) \cdot 10^3$
Bossart	0.7	$2 \times 11 \cdot 10^3$
LRF	0.2	254

<sup>6</sup> The error reduces if end corrections (elongation of the geometry) are applied in the LRF model.

This example showed the limitations of Bossart's model and the LRF model and that the SLNS model does not have these limitations. The SLNS model is accurate and 6.5 times faster than the FLNS model in this example.

#### 4.2 Condenser microphone

The second example is a condenser microphone. This is the same problem as described by Cutanda in his thesis on viscothermal acoustic BEM methods [7]. The model is axi-symmetric, although 3D models could have been made as well. This example model contains fluid structure interaction.

Figure 5 shows the condenser microphone very schematically. A flexible membrane under tension<sup>7</sup> is fixed at its round edge above a rigid plate. A uniform harmonic unit pressure is applied at the top of the membrane. This causes the membrane to displace inward and outward, squeezing air in and out of the layer through the opening at the circumference of the geometry. The radius of the membrane is 2mm, which is in the order of the acoustic length scale (and the mechanical length scale of the membrane). The layer of air below the membrane has a thickness of 18  $\mu\text{m}$  which is even lower than the characteristic viscous and thermal length scales (in the frequency range of interest).

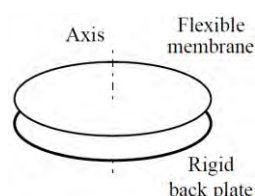


**Figure 5.** Schematic representation of the condenser microphone problem.

The microphone response, shown in Figure 6, is defined as the surface mean of the membrane deflection amplitude. The figure contains the results of three models: FLNS, SLNS and LRF. Bossart's model is not used because the air layer is too thin for this model. The differences between the responses of these models are too small to be distinguishable in the figure.

<sup>7</sup> Also the membrane is described by a Helmholtz equation.

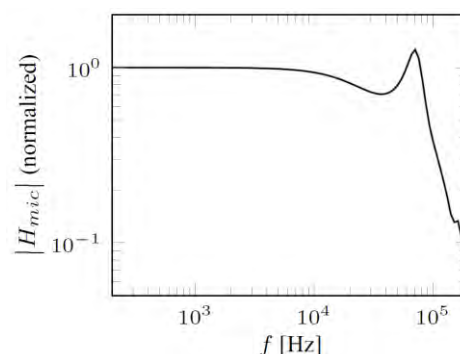


**Figure 6.** Modeled response of the microphone: FLNS, SLNS and LRF models.

The computational cost of the three models are listed in Table 2. Again, the SLNS model is faster than the FLNS model (using the same mesh), but the LRF model is the fastest, by far.

**Table 2.** Efficiency of the three microphone models.

Model	time [s]	# of DOFs
FLNS	0.6	7440
SLNS	0.25	4422+2412
LRF	0.01	402

This example showed that fluid structure interaction can be added to the models. The SLNS model is accurate and faster than the FLNS model, although the LRF model is the fastest for this example.

## 5. Discussion

This paper does not contain an example in which Bossart's model is accurate. The requirements for this model may even seem paradoxical: the geometry should be large enough, while viscothermal acoustic problems typically have small or narrow geometries. Although the range of problems for Bossart's is limited indeed, it can be very useful in some cases. Another impedance tube sample in which it is the preferred model is presented in [1,2].

In both examples, the SLNS model outperforms the FLNS model (which is equivalent to the model in COMSOL's thermoacoustics interface). Differences are even larger in 3D problems; see [1,2]. The SLNS model does however have some potential complications in fluid structure interaction problems; see [1,2]. In practice however, these complications can be ignored or circumvented in most, if not all cases. The

microphone example in this paper is a clear demonstration of this.

The LRF model is the fastest in all cases. Although this model is only applicable to narrow wave guides (layers and tubes), this geometry is typical for viscothermal acoustic problems, because it contains both the acoustic length scale, and the relatively small viscous and thermal length scales. The LRF model is often solved analytically. Nevertheless, it can be a very powerful model for FEM as well, especially if it can be easily coupled to other 3D (viscothermal) acoustic models.

The FLNS model is a set of PDEs that resembles the Navier-Stokes equations. The three reduced models on the other hand, are much more similar to the isentropic acoustic Helmholtz equation. The viscothermal effects in this analogy have the form of source terms: the viscous effect is a pressure gradient (velocity) dependent body force (dipole source), and the thermal effect is a pressure dependent mass inflow (monopole source). These sources are distributed over the boundary layer region in the SLNS model, lumped to the boundary in Bossart's model and lumped over the waveguide's cross-section in the LRF model. Coupling of the three reduced models to isentropic acoustics and to each other is very straightforward, because each uses a Helmholtz PDE of the pressure.

*COMSOL has made viscothermal acoustic modeling user friendly by providing the thermoacoustics interface. Hopefully, COMSOL will further pursue this course and consider the inclusion of more efficient models in future releases of the thermoacoustics interface.*

## 7. References

- [1] W.R. Kampinga, Y.H. Wijnant & A. de Boer, An Efficient Finite Element Model for Viscothermal Acoustics, *Acta Acustica united with Acustica*, **97**, 618-631 (2011).
- [2] W.R. Kampinga, Viscothermal acoustics using finite elements – analysis tools for engineers, *PhD thesis*, University of Twente (2010).
- [3] M.J.J. Nijhof, Viscothermal wave propagation, *PhD thesis*, University of Twente (2010).
- [4] R. Bossart, N. Joly & M.Bruneau, Hybrid numerical and analytical solutions for acoustic boundary problems in thermoviscous fluids, *Journal of Sound and Vibration*, **263**, 69-84 (2003).

[5] L.Cremer, Über die akustische Grenzschicht vor starren Wänden, *Archiv der elektrischen Übertragung*, **2**, 136-139 (1948).

[6] W.M. Beltman, Viscothermal wave propagation including acoustic-elastic interaction, *PhD thesis*, University of Twente (1998).

[7] V. Cutanda Henríquez, Numerical transducer modeling, *PhD thesis*, Technical university of Denmark (2002).

[8] W.R. Kampinga, Y.H. Wijnant & A. de Boer, Performance of several viscothermal acoustic finite elements, *Acta Acustica united with Acustica*, **96**, 115-124 (2010).

[9] F.J.M. van der Eerden, Noise reduction with coupled prismatic tubes, *PhD thesis*, University of Twente (2000).

## 8. Acknowledgement

The support of *Sonion* for this research is gratefully acknowledged.